Theoretical Applications of Jet Substructure: 1

Abhishek Iyer

JETS@LHC

27 January

Applications

tth, CP-properties di-higgs, W-tagging, non standard-jet

Q-G discrimination, Wavelets Vikram Rentala

New techniques Debajyoti Bardhan

Exotics-(extra-dimensions, Vector like fermions etc.) Ushoshi Maitra

SUSY- Sabyasachi Chakraborty

tth in the Standard Model

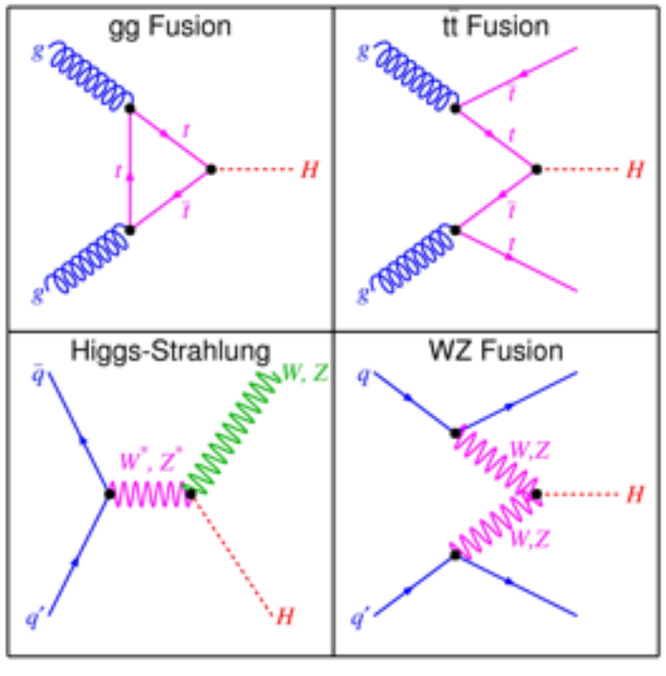

tt fusion channel gives a measure of the Top Yukawa

the gluon fusion channel for this purpose could be model dependent

Higgs is boosted more in this channel

Plehn, Salam, Spannowsky '09

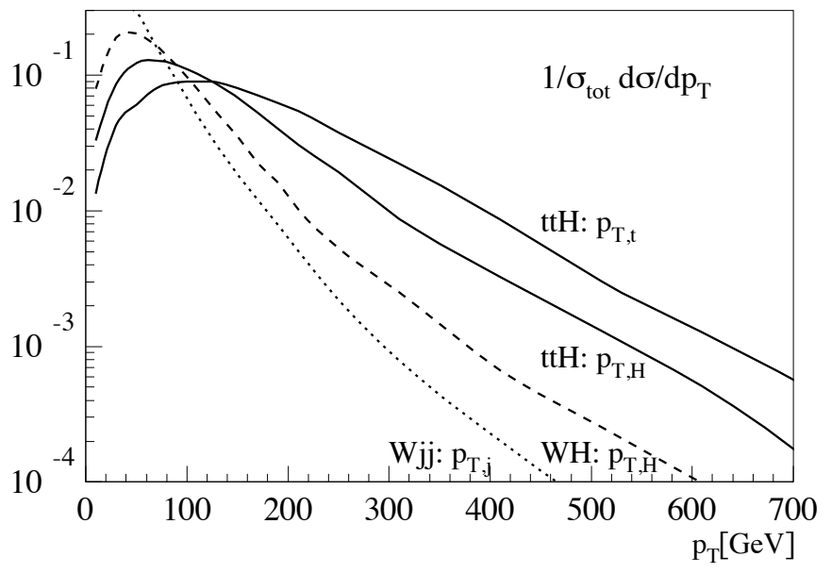

FIG. 1: Normalized top and Higgs transverse momentum spectra in $t\bar{t}H$ production (solid). We also show $p_{T,H}$ in W^-H production (dashed) and the p_T of the harder jet in W^-jj production with $p_{T,j} > 20$ GeV (dotted).

$pp \to t\bar{t}b\bar{b}$	irreducible QCD background
$pp \to t\bar{t}Z$	irreducible Z-peak background
$pp \to t\bar{t} + \text{jets}$	include fake bottoms

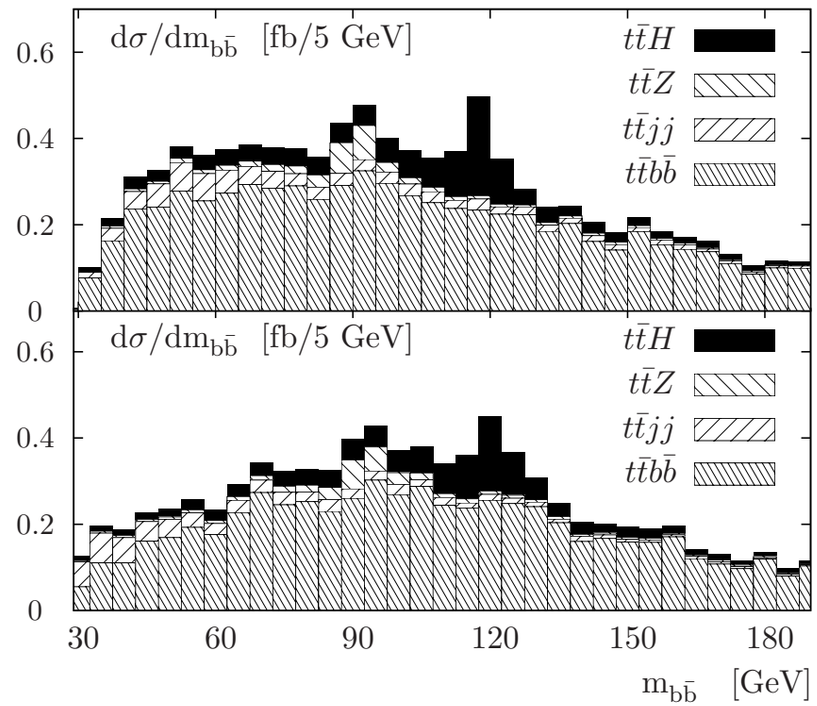

FIG. 3: Reconstructed bottom-pair mass m_{bb}^{rec} for signal ($m_H = 120$ GeV) and backgrounds without (upper) and including (lower) underlying event. The distributions shown include three b tags.

Measuring the signal strength in $t\bar{t}H$ with $H \to b\bar{b}$

Niccolo Moretti,[1,*] Petar Petrov,[2,†] Stefano Pozzorini,[1,‡] and Michael Spannowsky[2,§]

[1] *Physik-Institut, Universität Zürich, Winterthurerstrasse 190, CH-8057 Zürich, Switzerland*
[2] *Institute for Particle Physics Phenomenology, Department of Physics, Durham University, DH1 3LE, United Kingdom*

A precise measurement of the Higgs boson couplings to bottom and top quarks is of paramount importance during the upcoming LHC runs. We present a comprehensive analysis for the Higgs production process in association with a semi-leptonically decaying top-quark pair and subsequent Higgs boson decay into bottom quarks. Due to the highly complex final state and large Standard Model backgrounds, measuring the signal strength in this process is known to be challenging. To maximise the sensitivity, we analyse different, statistically independent, phase space regions, where one or more of the heavy resonances are boosted. This allows us to employ jet substructure techniques, which help to reduce large $t\bar{t} + \text{X}$ backgrounds. We find that combining several $t\bar{t}H(b\bar{b})$ phase space regions will allow one to measure deviations of the Standard Model signal strength of order 20% with $3\,\text{ab}^{-1}$.

Christoph Englert, Emmanuel Re '14

Top Yukawa through thj

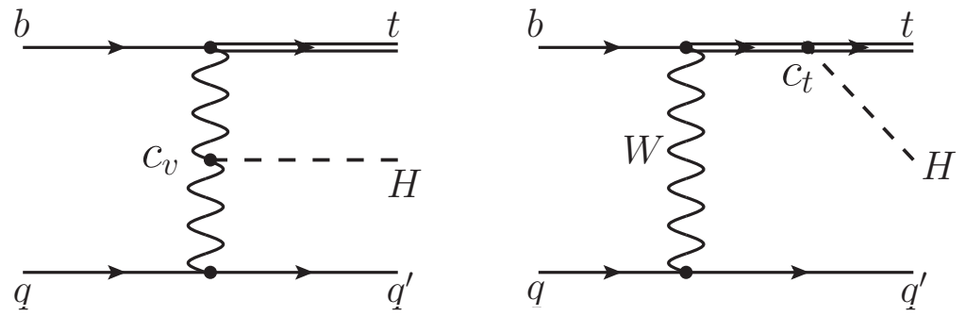

FIG. 1: Feynman diagrams for tree-level production of single-top + Higgs. The diagram on the left (right) is proportional to C_{WWH} (C_{ttH}).

$$C_{ttH}^{\rm SM} = -\frac{y_t}{\sqrt{2}} = -\frac{m_t}{v_{\rm SM}}\,, \qquad C_{WWH}^{\rm SM} = g_W^2\frac{v_{\rm SM}}{2} \tag{1}$$

as

$$C_{ttH} = c_t \times C_{ttH}^{\rm SM}\,, \qquad C_{WWH} = c_v \times C_{WWH}^{\rm SM}\,. \tag{2}$$

Constructive or destructive interference depending on the sign of top Yukawa

Larger value could result in different decay patterns (right tops)

Photon decay mode of the Higgs is considered

$y_t \geq 0.5 y_t^{SM}$ 95 pc CL at HL LHC

Measurement of bottom coupling

Englert, Mattelaer, Spannowsky '16

Higgs production through WBF

Combination of jet substructure and matrix element techniques in the boosted regime

Divide the events into a fat jet and a tagging jet

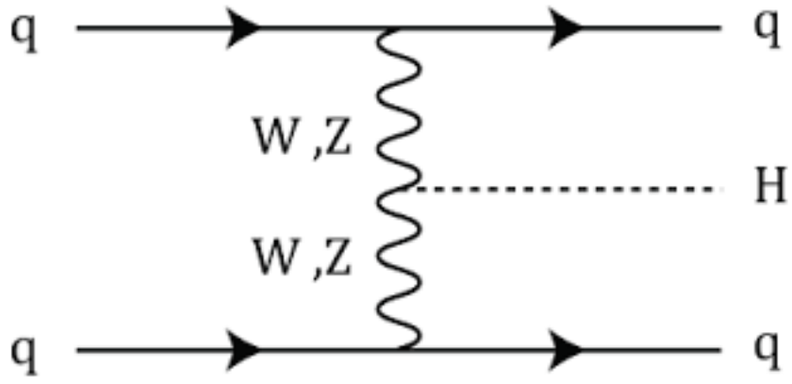

Normal kinematic handles are not useful in reducing backgrounds

Matrix Element method

Shower deconstruction

Projecting to 600 fb^{-1}, we obtain a con-

$$0.82 < y_b/y_b^{\mathrm{SM}} < 1.14$$

Godbole, Miller, Mohan, White '13, '15

Boosting Higgs CP properties

$$g_W^2 \frac{c_1}{2\Lambda_1^2} \Phi^\dagger \Phi \, F_{\mu\nu} \, F^{\mu\nu}, \quad g_W^2 \frac{c_2}{2\Lambda_2^2} \Phi^\dagger \Phi \, \tilde{F}_{\mu\nu} \, F^{\mu\nu},$$

Modifications to the HVV vertex

Distinguish using angular observables

$$\cos\theta^* = \frac{\vec{p}_{l_1}^{(V)} \cdot \vec{p}_V}{|\vec{p}_{l_1}^{(V)}|\,|\vec{p}_V|}, \quad \cos\delta^+ = \frac{\vec{p}_{l_1}^{(V)} \cdot (\vec{p}_V \times \vec{p}_H)}{|\vec{p}_{l_1}^{(V)}|\,|\vec{p}_V \times \vec{p}_H|},$$

$$\cos\delta^- = \frac{(\vec{p}_{l_1}^{(H-)} \times \vec{p}_{l_2}^{(H-)}) \cdot \vec{p}_V}{|(\vec{p}_{l_1}^{(H-)} \times \vec{p}_{l_2}^{(H-)})||\vec{p}_V|}.$$

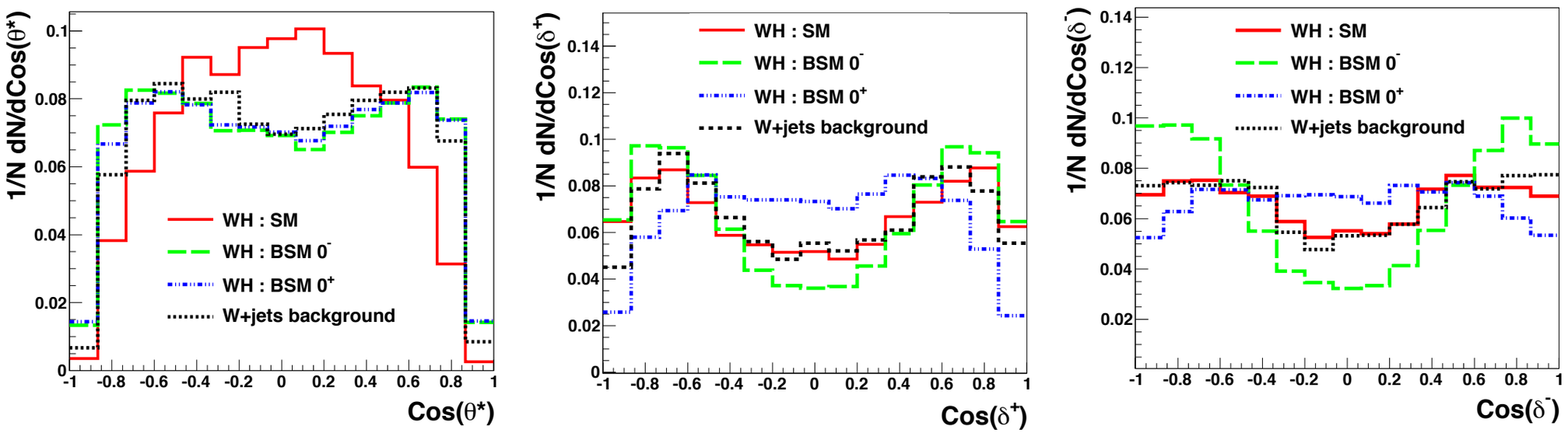

(a) (b) (c)

FIG. 2. Distributions of the angles defined in eq. (4) for WH production in the SM (solid red lines), pure BSM CP even (dot-dashed blue lines), pure BSM CP odd (dashed green lines) and for the dominant W + jets background (dotted black lines). (a) $\cos\theta^*$, (b) $\cos\delta^+$ (c) $\cos\delta^-$, constructed with the BT algorithm.

Godbole, Miller, Mohan, White '13, '15

$$A(X) = \frac{\sigma(|X| < 0.5) - \sigma(|X| > 0.5)}{\sigma(|X| < 0.5) + \sigma(|X| > 0.5)}$$

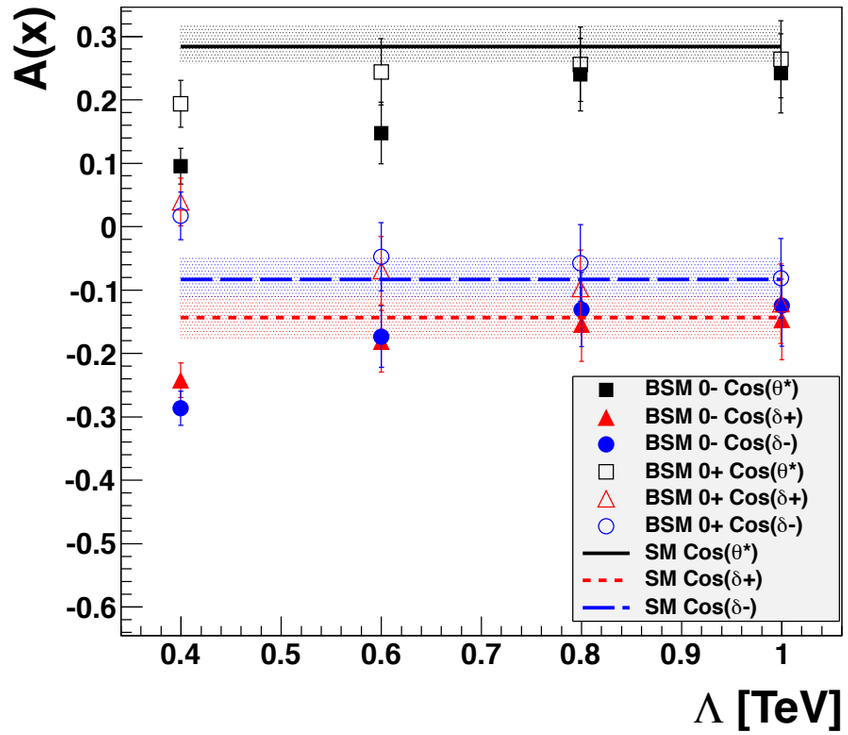

FIG. 3. The value of the asymmetries defined in eq. (5) for the CPC and CPV scenarios for WH production, constructed with the BT algorithm. The strength of the BSM contribution is varied through the parameters Λ_i. The horizontal lines indicate the asymmetry in the SM. The contribution from the dominant Wjj background is included in the evaluation of these asymmetries. The statistical uncertainty in the determination of these asymmetries for $300\,\text{fb}^{-1}$ of data for 14 TeV LHC is shown by the shaded regions for SM and by the error bars for BSM scenarios.

Boosting the Direct CP Measurement of the Higgs-Top Coupling

Matthew R. Buckley
Department of Physics and Astronomy, Rutgers University, Piscataway, NJ 08854, USA

Dorival Gonçalves
Institute for Particle Physics Phenomenology, Department of Physics, Durham University, UK

We parametrize the top-Higgs interaction as

$$\mathcal{L} \supseteq -\frac{m_t}{v} K \bar{t} \left(\cos\alpha + i\gamma_5 \sin\alpha\right) t \; H,$$

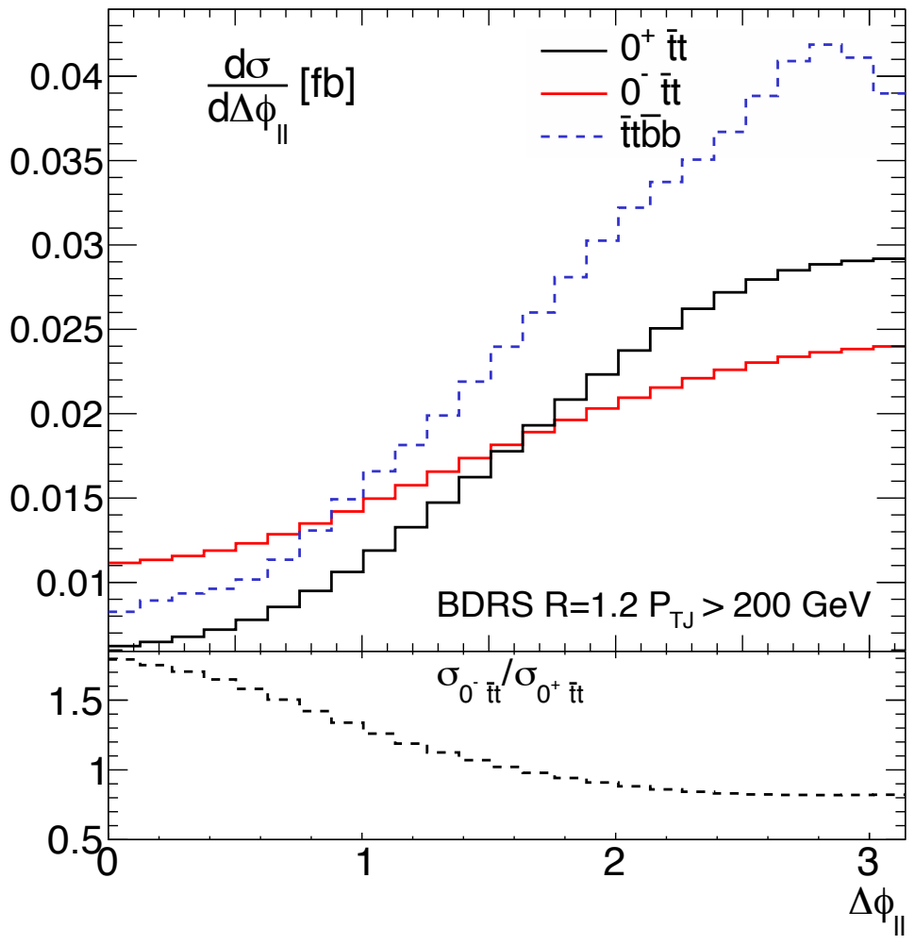

FIG. 3. Azimuthal correlation between the two leptons $\Delta\phi_{\ell\ell}$ calculated in the lab-frame after the BDRS analysis.

di-higgs in the SM

di Lima, Papaefstathiou, Spannowsky '14

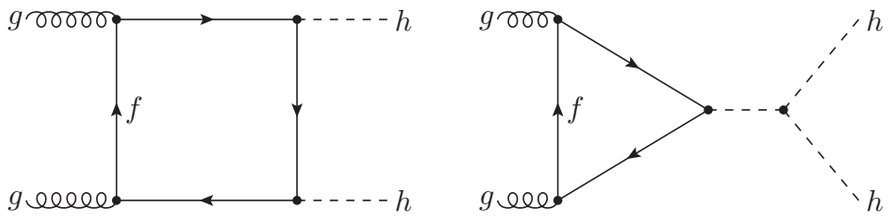

Figure 1: Higgs boson pair production diagrams contributing to the gluon fusion process at LO are shown for a fermion f. These are generic diagrams and therefore, do not include all permutations.

pT of Higgs for full process

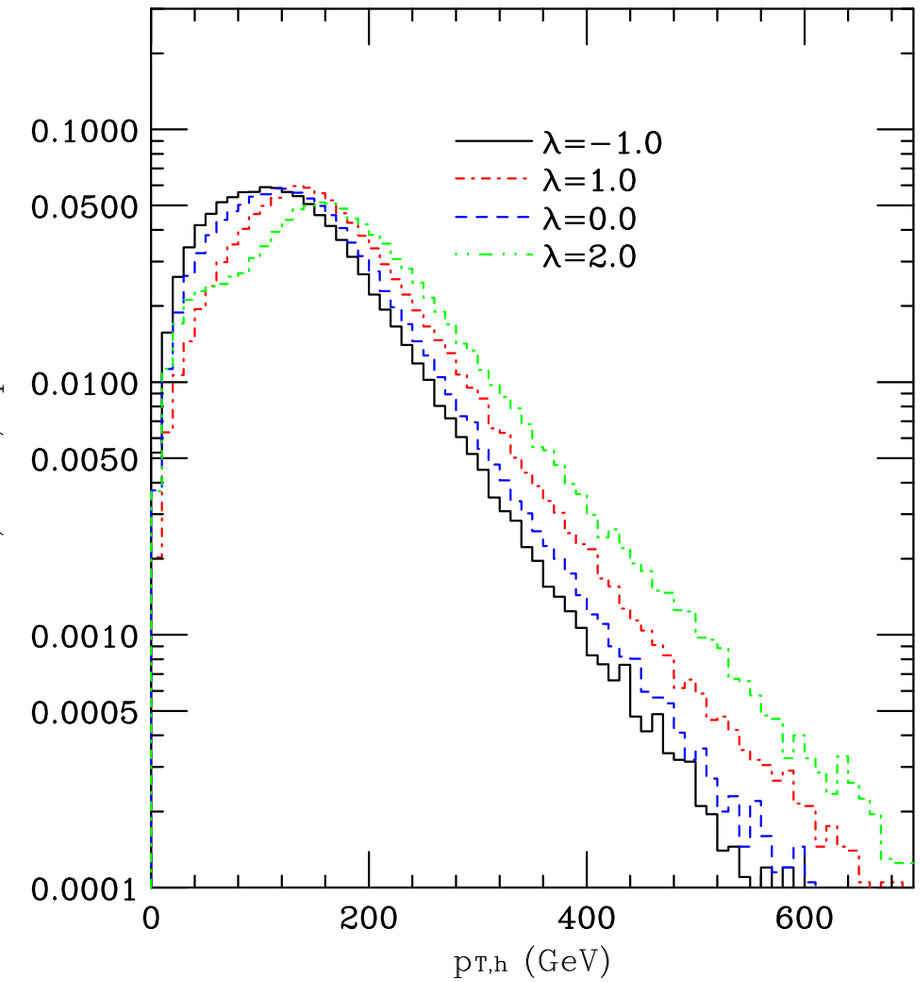

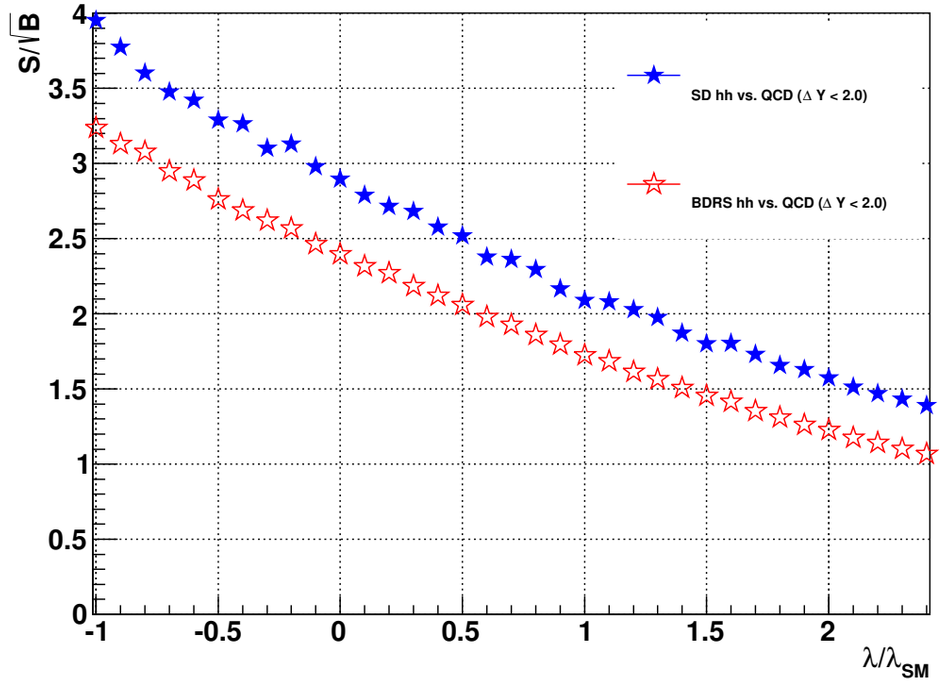

Figure 8: The best expected significance of the different Higgs tagger methods for different values of λ at 3000 fb^{-1} for a 14 TeV LHC.

$$\lambda \leq 1.2 @\ 95\% \text{C.L.}$$

Improving with multivariate techniques

- N-Subjettiness
- Energy-Correlations
- kt-dist measure

$$\sqrt{d_{12}} \equiv \min\left(p_{T,1}, p_{T,2}\right) \cdot \Delta R_{12}\,.$$

Behr et al. '16

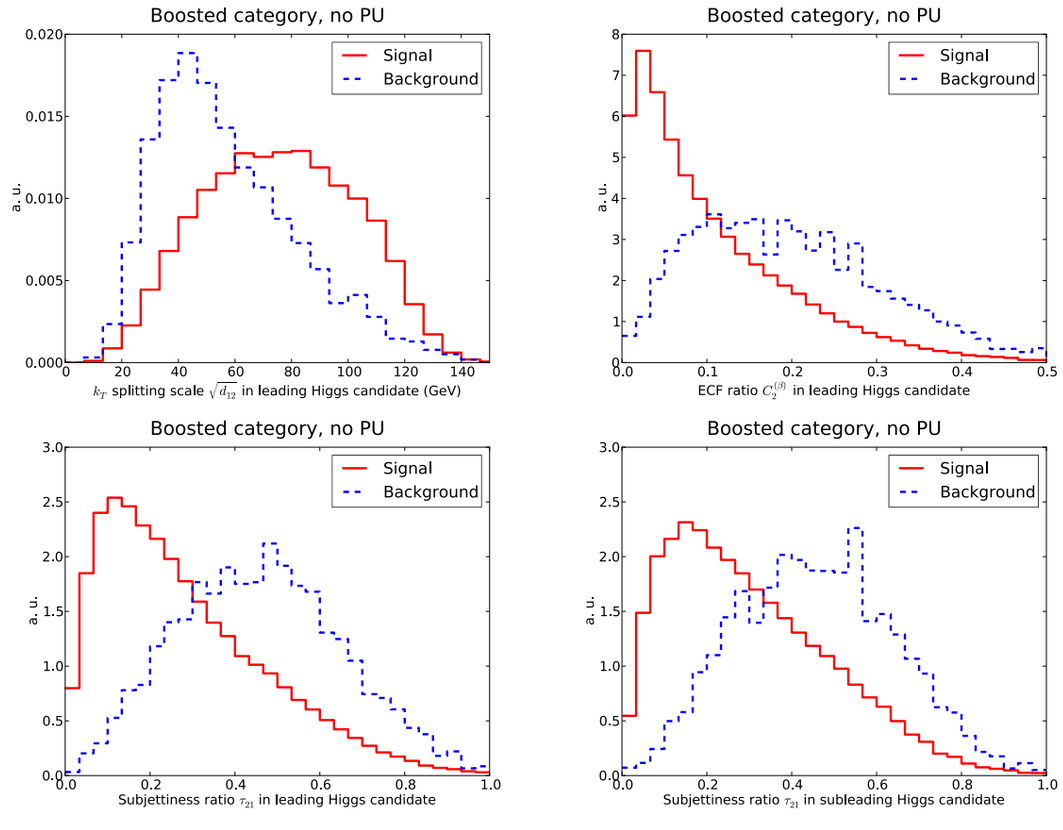

Figure 8: Distribution of representative substructure variables in the boosted category at the end of the cut-based analysis, to be used as input to the MVA. From top to bottom and from left to right we show the k_t splitting scale $\sqrt{d_{12}}$, the energy correlation ratio $C_2^{(\beta)}$ and the subjettiness ratio τ_{21} for the leading Higgs. In the case of τ_{21} the distributions for the subleading Higgs are also given.

Significance of 3 standard deviations at 3 ab^-1

di-higgs in the NP Searches for TeV scale resonances

Cooper, Konstantinidis, Lambourne, Wardrope '16

Graviton Mass [GeV]	$\sigma(pp \to G_{\rm KK} \to hh \to b\bar{b}b\bar{b})$ [fb]	Γ [GeV]
500	329	18.6
700	72.7	33.9
900	18.6	48.6
1100	5.51	62.7
1300	1.82	76.5
1500	0.65	90.0

Analysis can also be extended to ZH-4b, ZZ-4b

Falkowski, Krohn, Wang, Shelton, Thallpillil '10

Pre-higgs era

higgs to gluons

h-2scalars-4 gluons

Now:NP through Higgs?

$$\overline{m} \equiv \frac{m(j_1) + m(j_2)}{2} < 10 \text{ GeV},$$

$$\alpha = \min\left[\frac{m(j_1)}{m(j_2)}, \frac{m(j_2)}{m(j_1)}\right]$$

$$\beta = \frac{p_T(j_3)}{p_T(j_1) + p_T(j_2)},$$

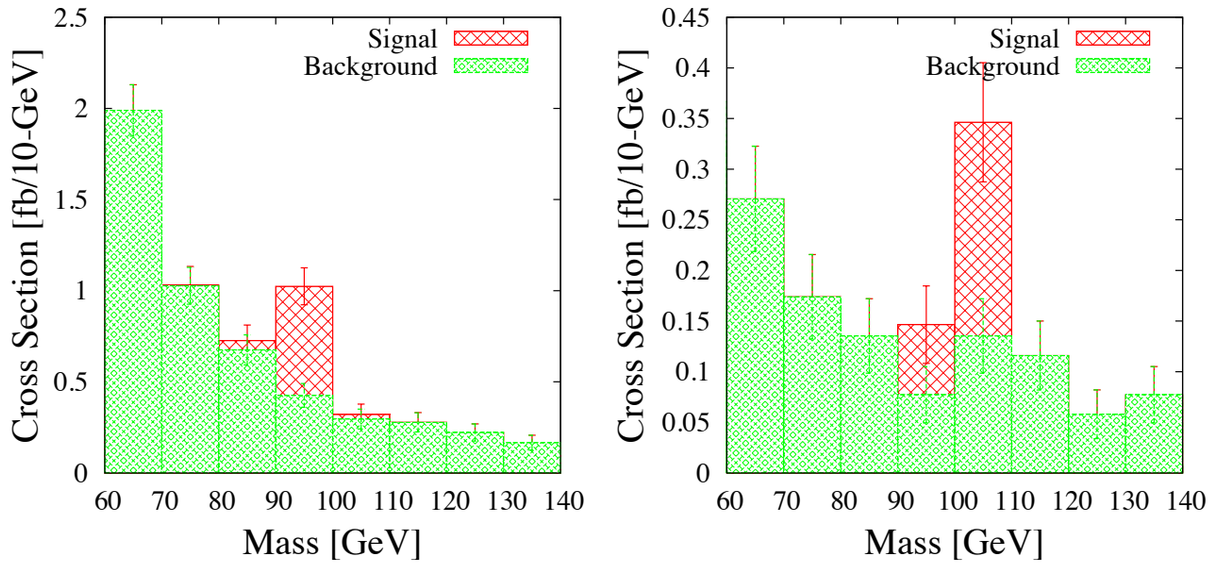

FIG. 1: Reconstructed $m_H = 100$ GeV Higgs mass (left) in the $V + h$ channel, after the cuts of Table I (excluding the cut on m_H); (right) in the $t\bar{t}+h$ channel, after the cuts of Table II (excluding the cut on m_H). Error bars show statistical errors.

Kribs, Martin, Roy, Spannowsky '09

Pre-higgs era

$$p + p \;\rightarrow\; \chi_1 + \chi_1 + \text{anything} \;\rightarrow\; h + \gamma + X + \not{E}_T \;,$$

Now:NP through Higgs?

$$\not{E}_T > 100 \text{ GeV} \qquad p_t^\gamma > 100 \text{ GeV} \qquad p_t^b > 200 \text{ GeV}$$

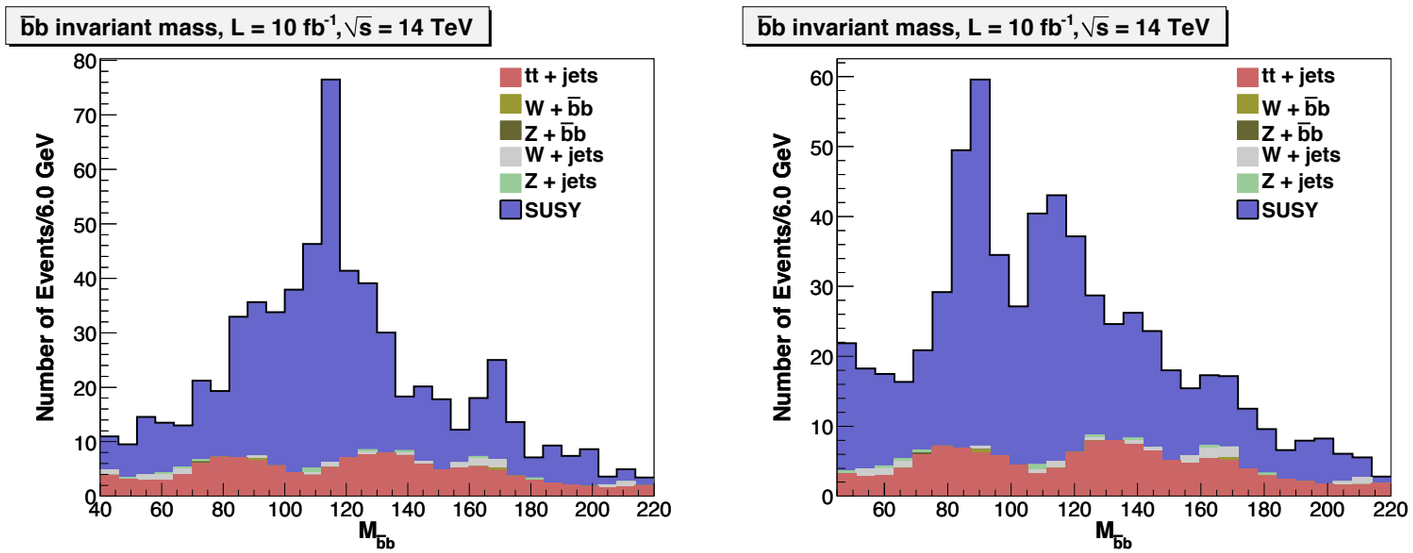

FIG. 1: The Higgs peak in the $b\bar{b}$ invariant mass distribution is easily resolved above the supersymmetric and standard model backgrounds, and well separated from the Z peak, using our jet substructure algorithm. The left figure (a) corresponds to "Point 1" (Higgsino NLSP) while the right figure (b) corresponds to "Point 2" (Bino NLSP). See text for details. (color online)

Cui, Han, Schwartz '11

W-tagging

Earlier methods applied traditional grooming/mass drop to identify the W candidate

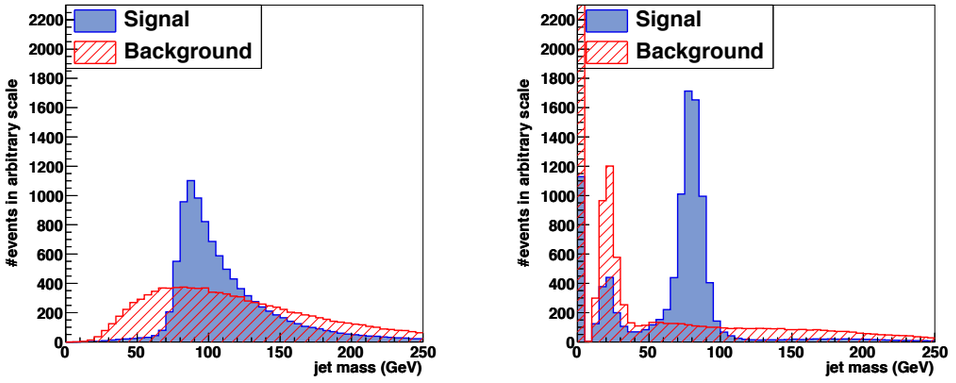

(a) (b)

FIG. 2: Jet masses before and after filtering/mass-drop for $p_T^{\text{jet}} \in (500, 550)$ GeV. The numbers of events are normalized to be the same for the signal and the background. (a) Before filtering; (b) after filtering with $\mu = 0.71$ and $y_{\text{cut}} = 0.09$. When a mass-drop is not found, we add an entry in the zero mass bin such that the total number of jets is unchanged.

These techniques gave ~ 2 in the S/sqrt{B}

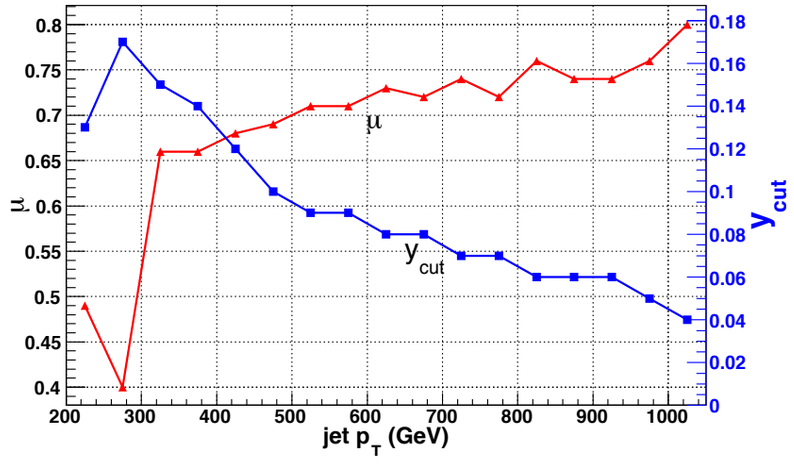

(a) Optimized filtering parameters

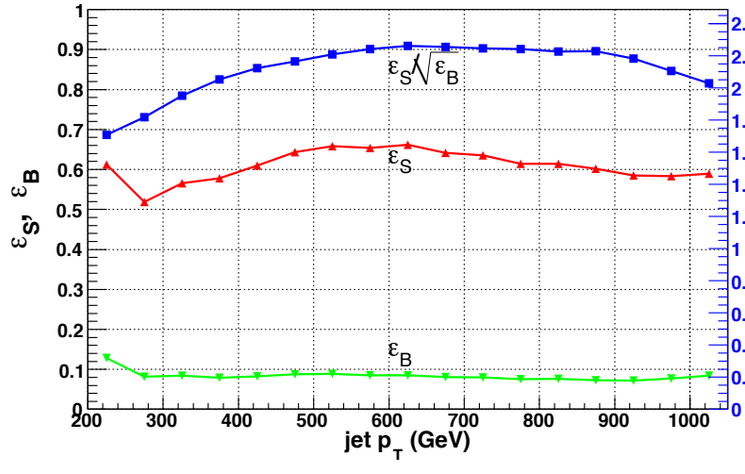

(b) Optimized filtering efficiences and S

- Recluster the fat-jet with a smaller $R < R_{\rm fat}$.
- Take the highest p_T subjet after reclustering, call its mass $m(R)$ and its transverse momentum $p_T(R)$.
- The **mass *R*-cores** are defined as $c_m(R) \equiv m(R)/m(R_{\rm fat})$.
- The **$\mathbf{p_T}$ *R*-cores** are defined as $c_{p_T}(R) \equiv p_T(R)/p_T(R_{\rm fat})$.

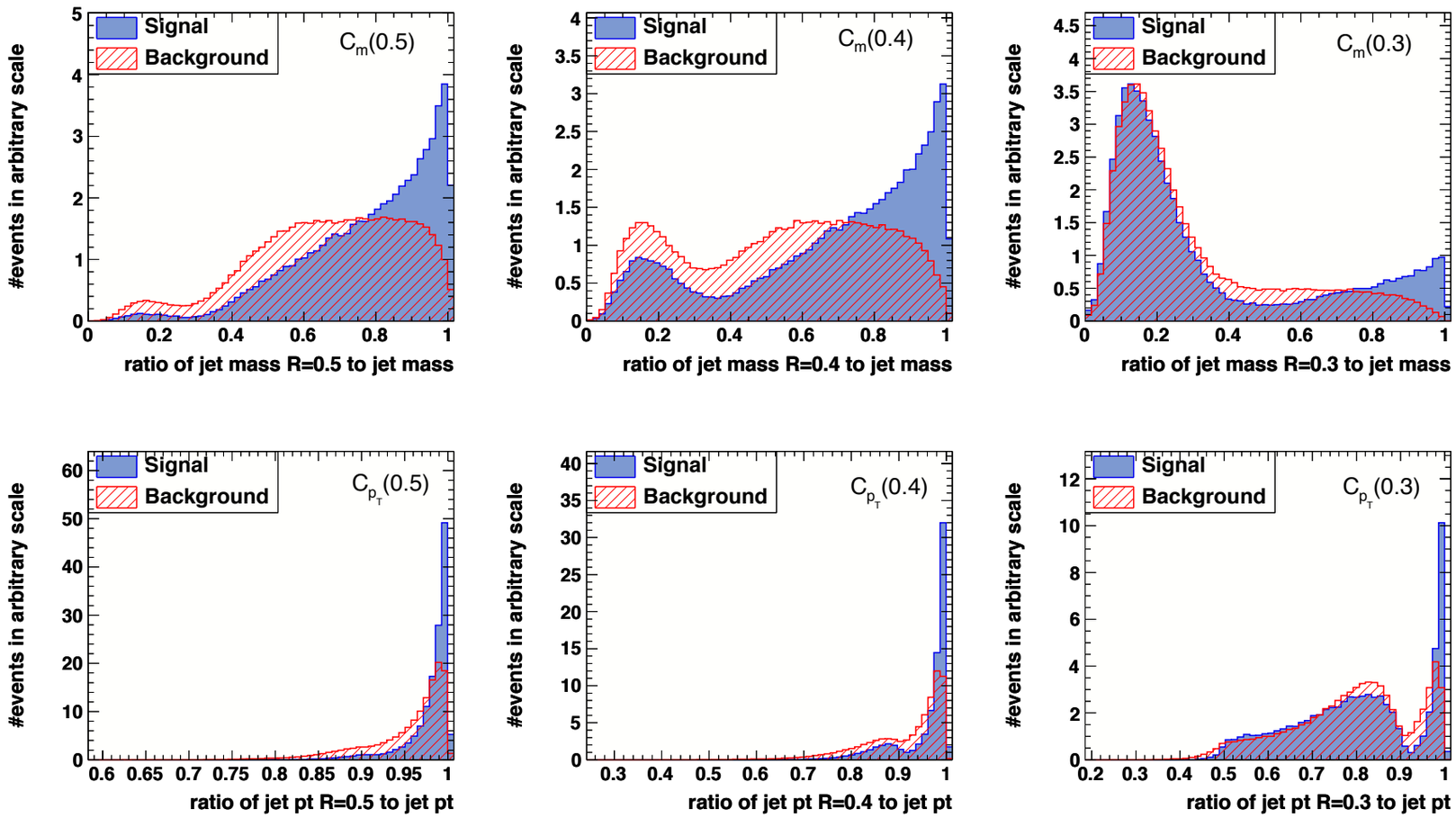

FIG. 6: Representative R-core distributions for $R = 1.2$ fat jets with $p_T^{\rm jet} \in (500, 550)$ GeV and $m_{\rm filt} \in (60, 100)$ GeV. A dissection of the physics producing these shapes is discussed in the text.

Cui, Han, Schwartz '11

$$\text{sens}^m_{\text{filt}} \equiv \frac{m_{\text{filt}}}{m}, \qquad \text{sens}^m_{\text{trim}} \equiv \frac{m_{\text{trim}}}{m}, \qquad \text{sens}^m_{\text{prun}} \equiv \frac{m_{\text{prun}}}{m},$$

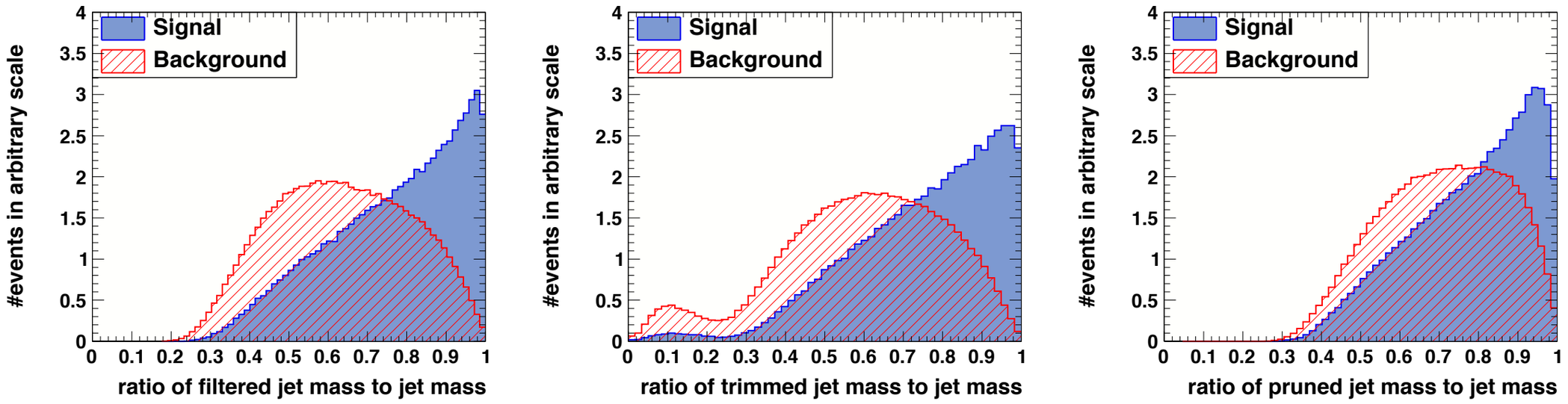

FIG. 11: Distributions of grooming sensitivities, $\text{sens}^m_{\text{filt}}$, $\text{sens}^m_{\text{trim}}$, and $\text{sens}^m_{\text{prun}}$ for signal (W-jets) and background (QCD-jets) for $p_T^{\text{jet}} \in (500, 550)$ GeV. All events satisfy $m_{\text{filt}} \in (60, 100)$ GeV.

Cui, Han, Schwartz '11

Planar Flow

Define a matrix

$$I_w^{kl} = \frac{1}{m_{\rm jet}} \sum_i w_i \frac{p_{i,k}}{w_i} \frac{p_{i,l}}{w_i}$$

$$P_f = \frac{4det(I_w)}{tr(I_w)^2} = \frac{4\lambda_1\lambda_2}{(\lambda_1+\lambda_2)^2}$$

0 for linear distributions and 1 for isotropic distributions

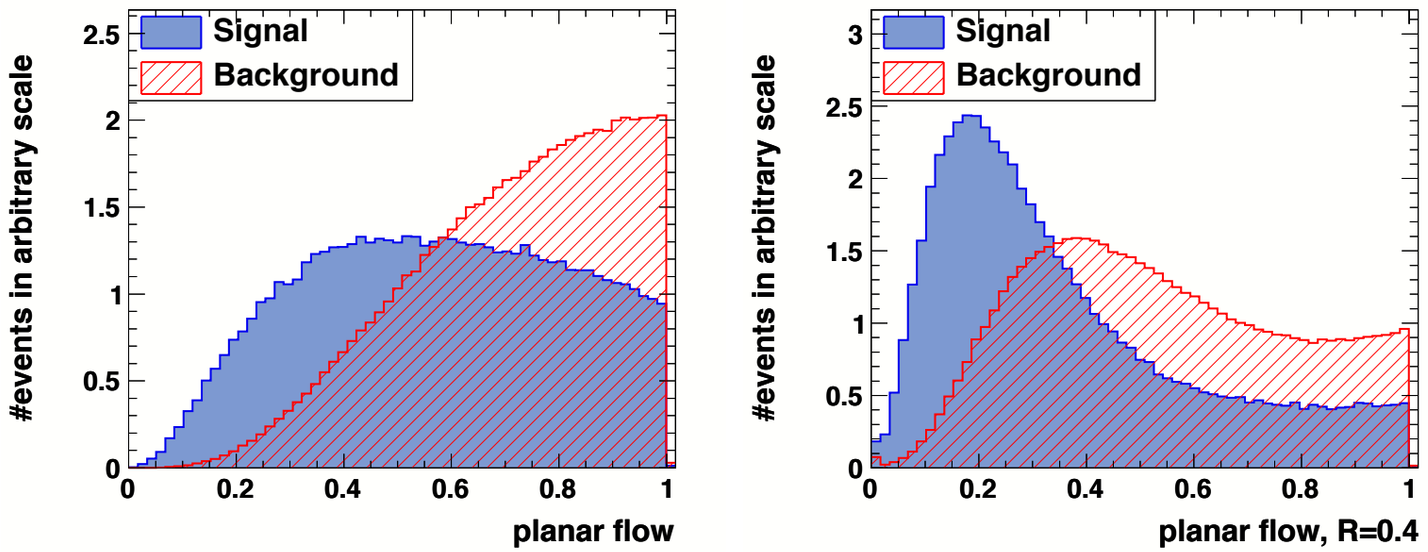

(a) (b)

FIG. 12: Signal vs. background planar flow (P_f) distributions for $p_T^{\rm jet} \in (500, 550)$ GeV: (a) P_f for the fat jet ($R = 1.2$); (b) P_f for the leading subjet reclustered with $R = 0.4$.

Cui, Han, Schwartz '11

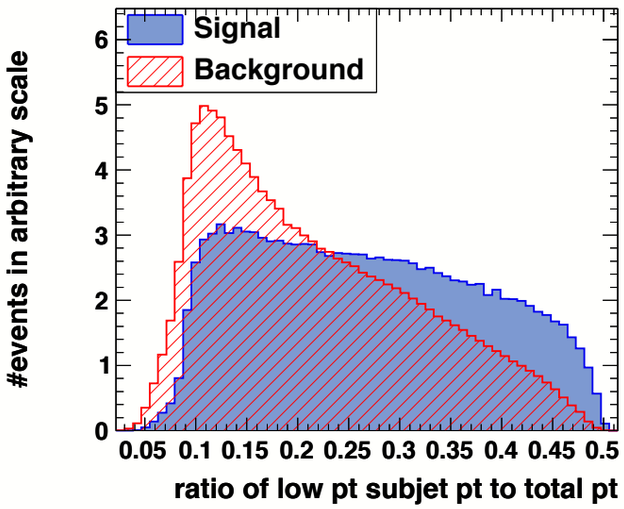

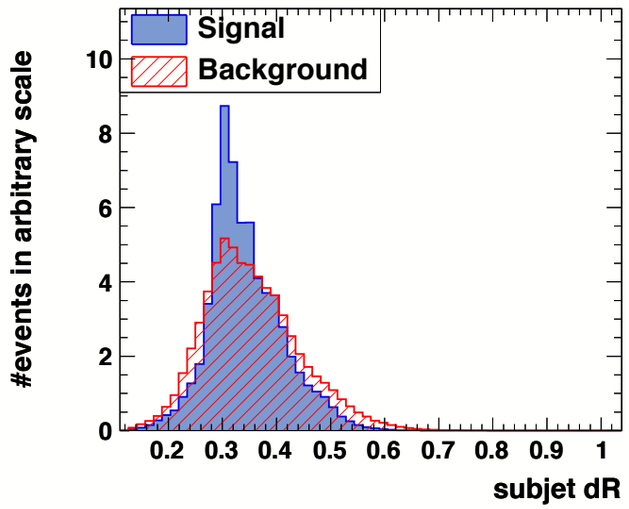

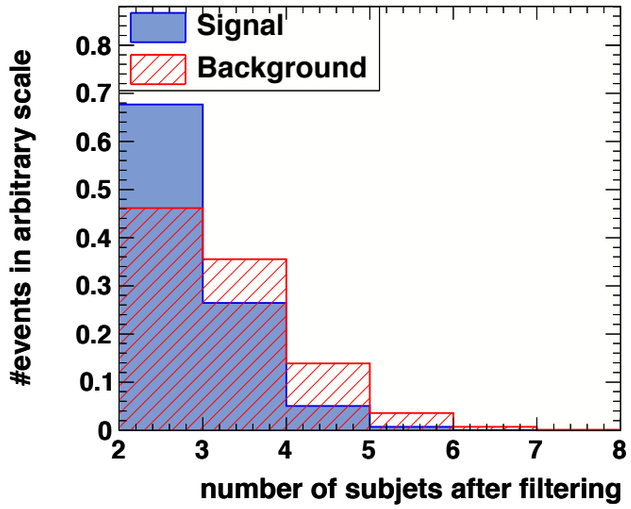

Then do a MVA

$$m_{\rm jet},\ c_{p_T}(0.2-0.11),\ {\rm sens}^{m,p_T}_{\rm filt,trim,prun},\ P_f,\ P_f(0.4),\ \frac{p_T^{\rm sub1,sub2}}{p_T},\ \frac{m^{\rm sub1,sub2}}{m},\ \Delta R_{\rm sub},\ n_{\rm sub}.$$

A factor 5 improvement
in the tagging efficiency

Applications of W-tagging

WW-scattering (SM+NP) Cui, Han ' 13

Boosted di-boson resonances (any NP you like)

Anything else you can think of

Englert, Roy, Spannowsky '11

di-tau jets

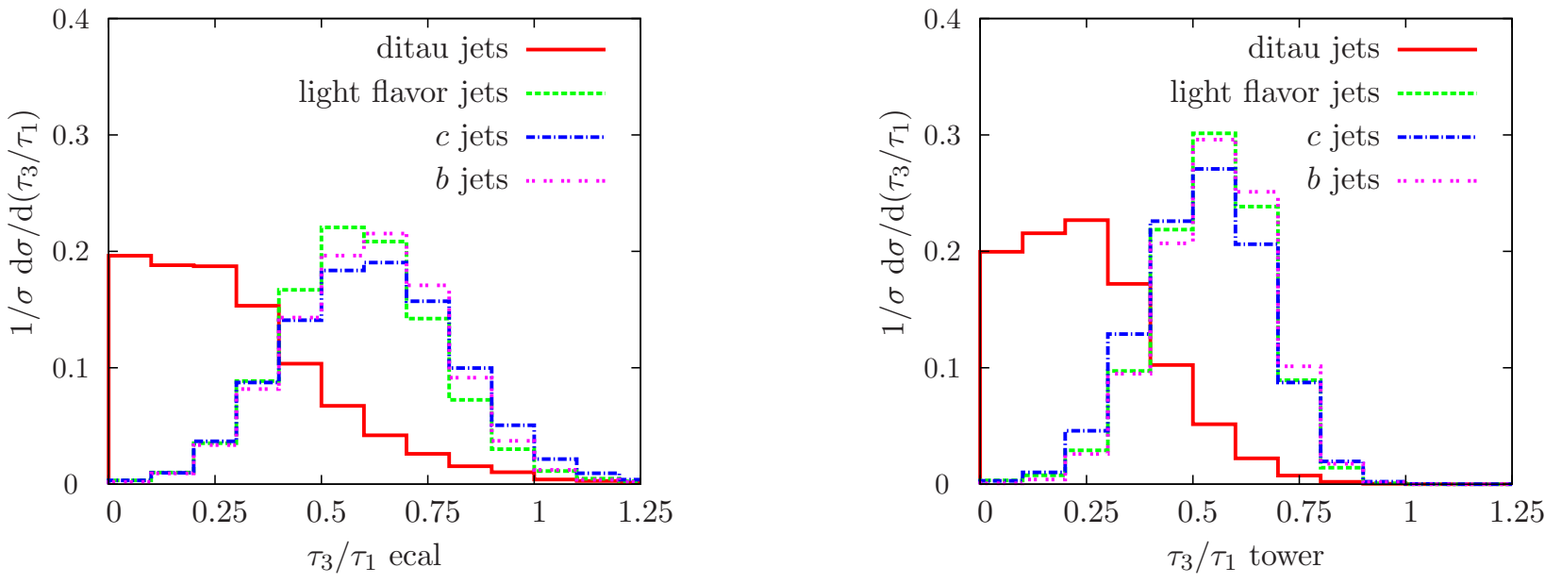

FIG. 3: Normalized differential distributions of the N-subjettiness ratio τ_3/τ_1. In the left panel we plot this ratio for ecal hits only, and in the right panel we plot τ_3/τ_1 for the full calorimeter tower entries.

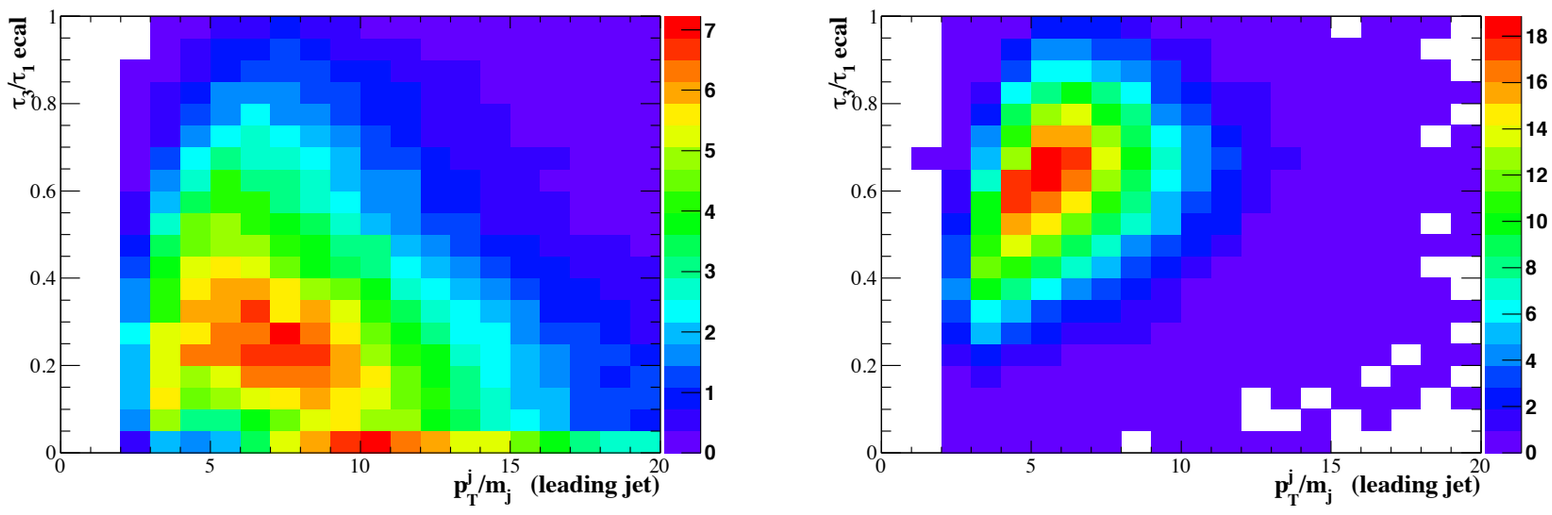

FIG. 4: Two-dimensional distribution of 10^3 signal events (left panel) and 10^3 b jet events in the τ_3/τ_1–p_T^j/m_j plane. The ditau events are less correlated than QCD jets.

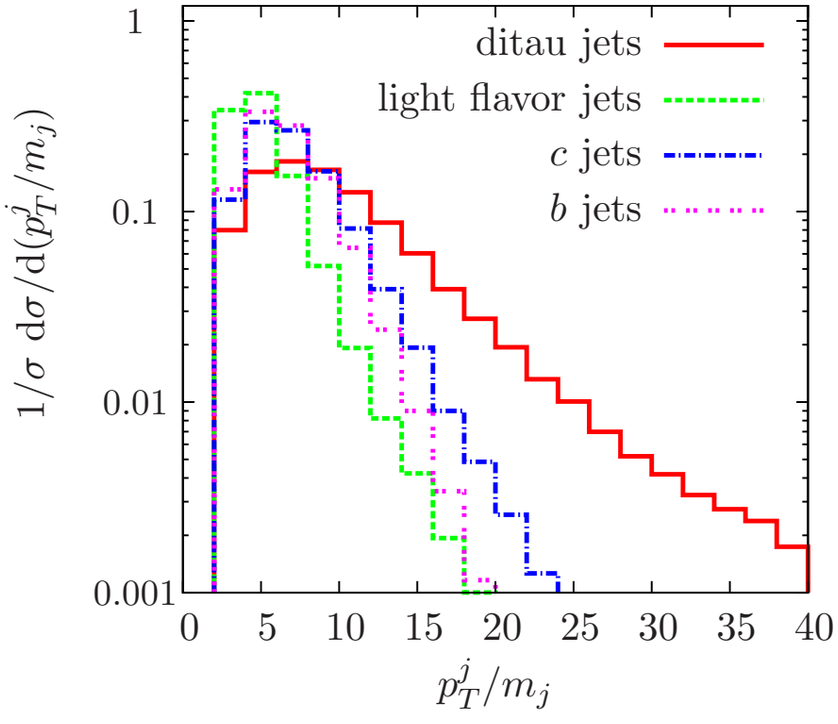

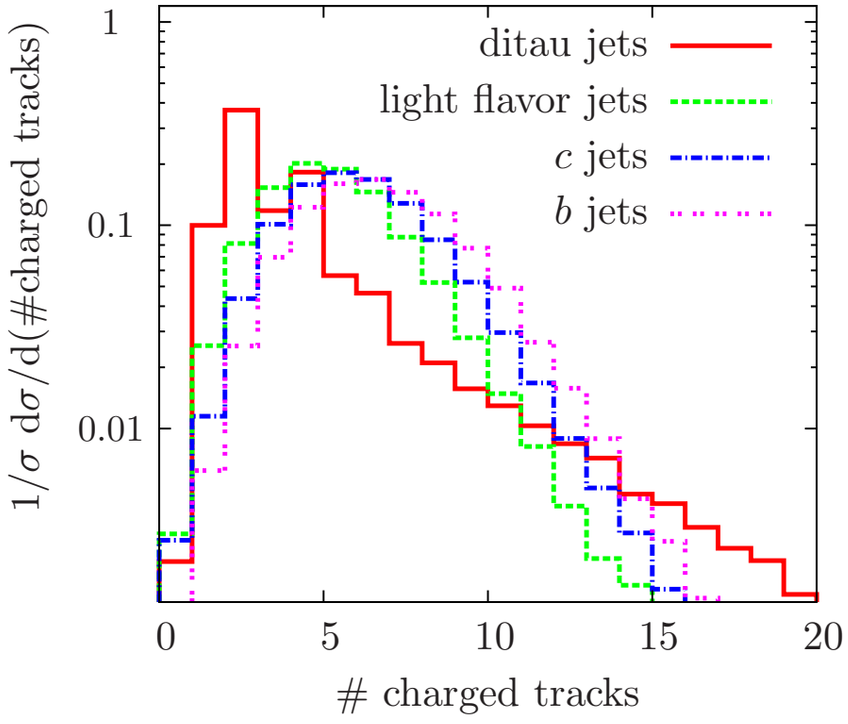

$$L = f\left(\tau_3/\tau_1|_{\mathrm{ecal}}\right) \times f(p_T^j/m_j) \times f(\text{charged tracks})$$

$$d = p(\text{light flavor})\,\frac{L(\text{ditau})}{L(\text{ditau}) + L(\text{light flavor})} + p(c)\,\frac{L(\text{ditau})}{L(\text{ditau}) + L(c)} + p(b)\,\frac{L(\text{ditau})}{L(\text{ditau}) + L(b)}\,.$$

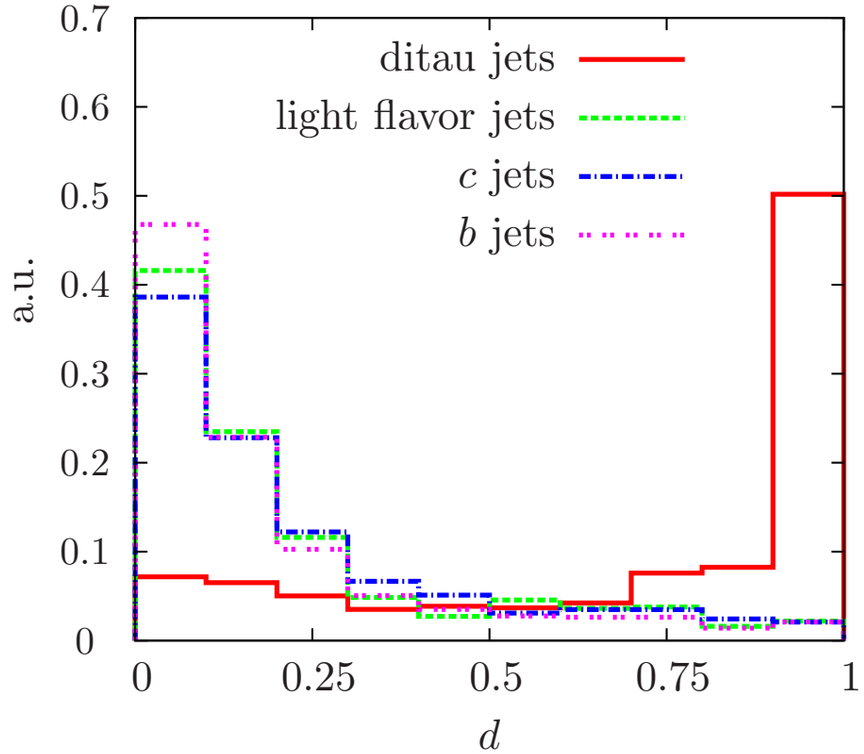

Tagging ditau (all hadronic) jets

We perform a series of quantitative studies:

- use the decay channel: $h \rightarrow a(\tau\tau)a(\tau\tau)$
- for ditau jets we use: $m_a = 10\ \mathrm{GeV}$
- for background jets we use jets in QCD dijet events

Some example S/B distributions:

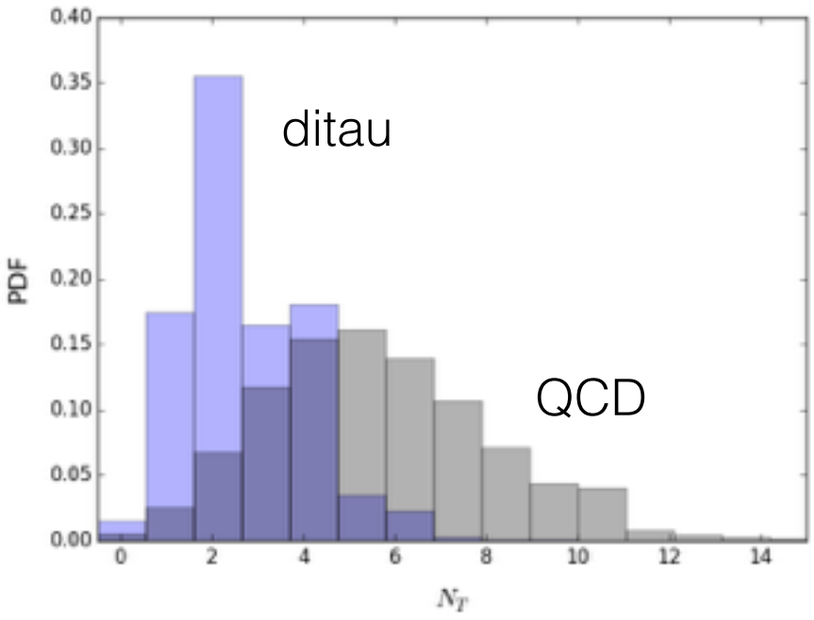

ditau

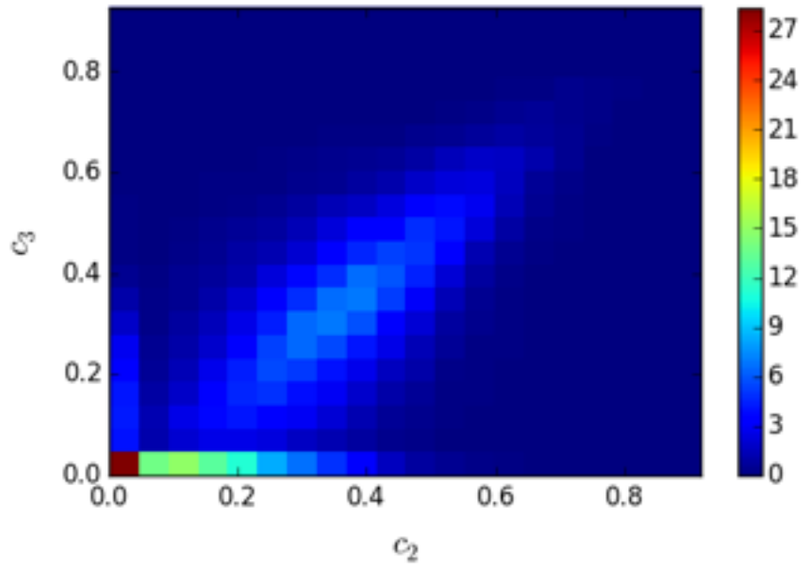

QCD

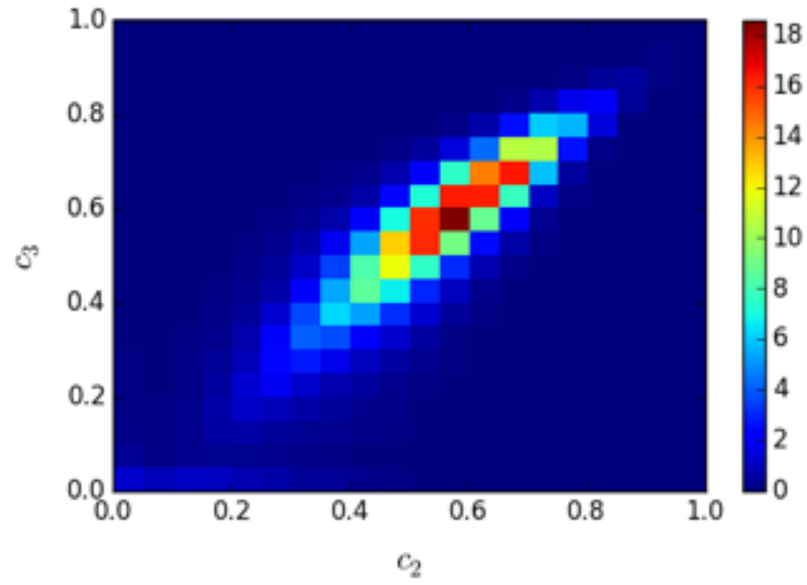

Non standard jets

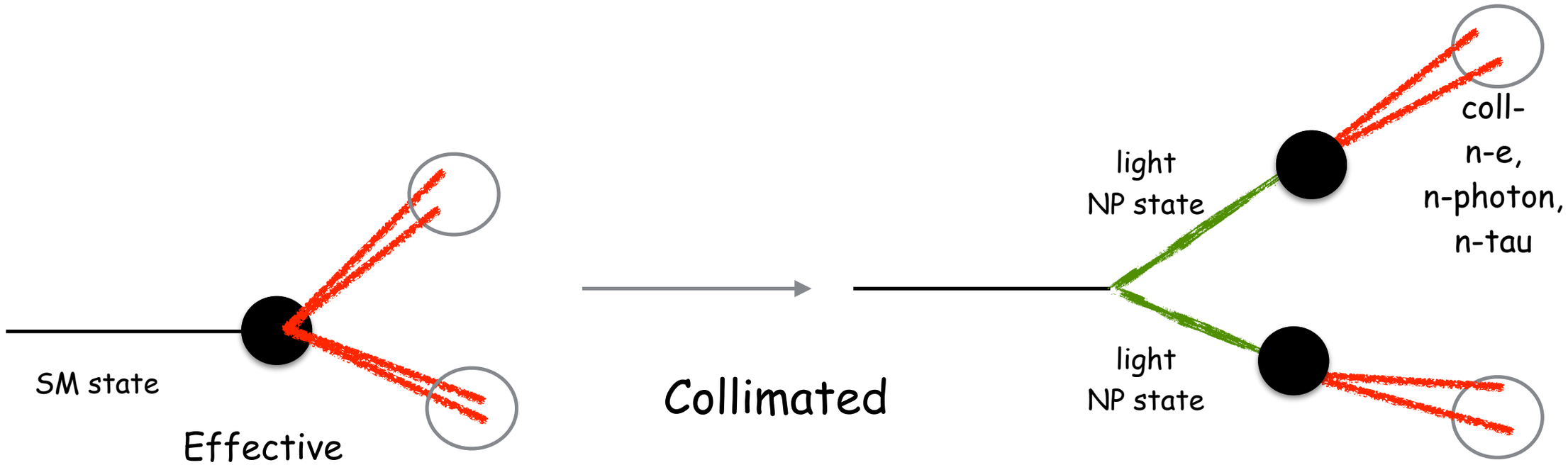

They look like 2 e, 2 photon, 2 tau final state

Note: e, photons are not point like but have a spread in the $\eta - \phi$ direction

Ellis, Roy Scholtz '12

$$\lambda_J = \log\left(1 - \frac{p_{T_L}}{p_{T_J}}\right)$$

$$\epsilon_J = \frac{E_L\left(E_{NL} + E_{NNL}\right) + E_{NL}E_{NNL}}{E_J^2}$$

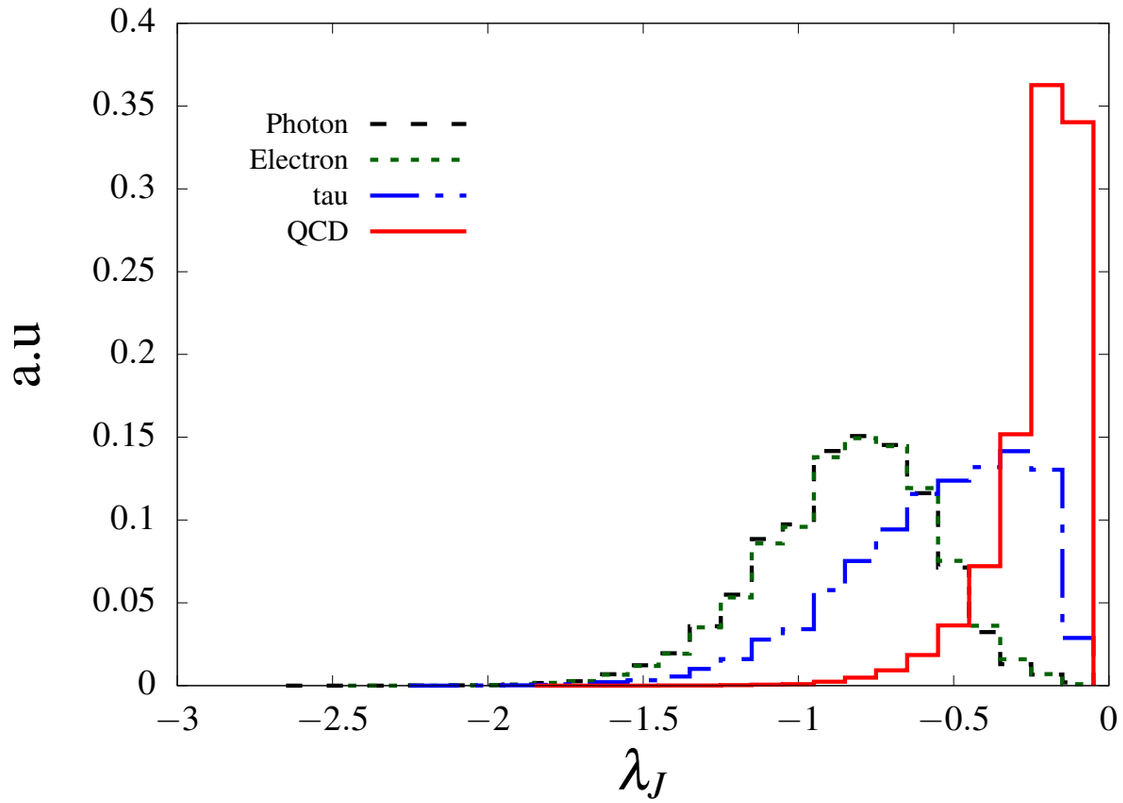

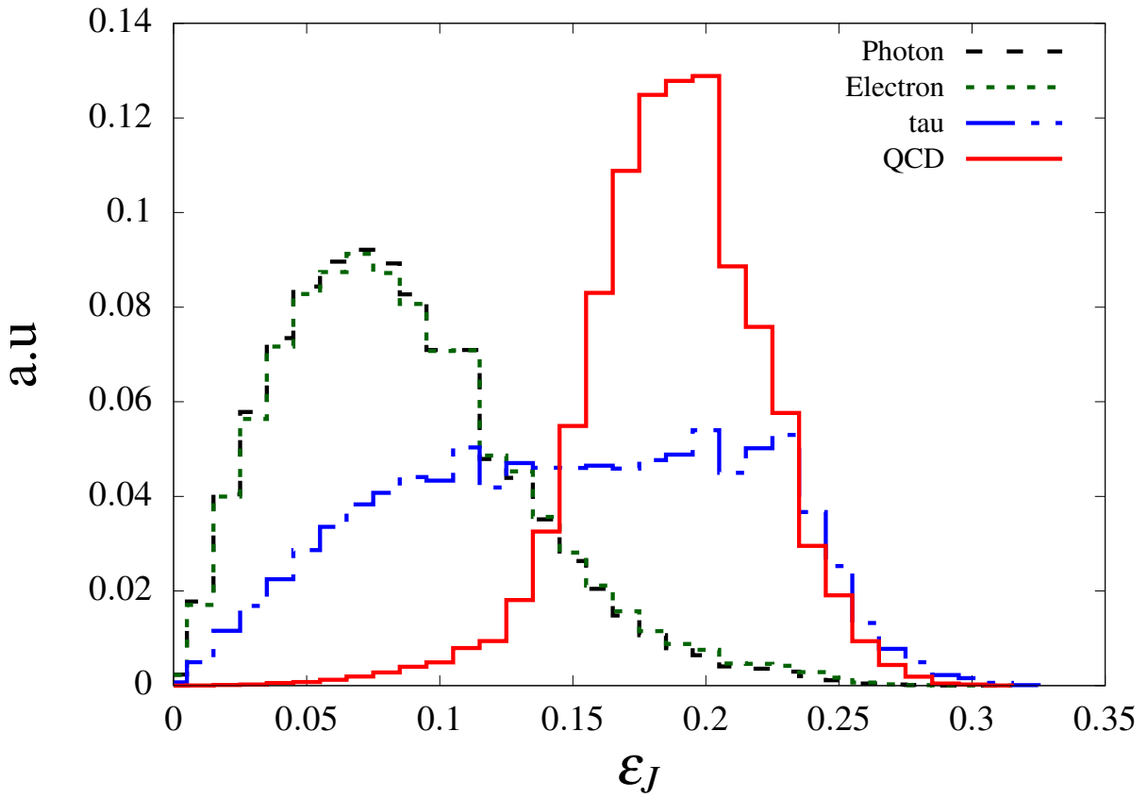

Ellis, Roy Scholtz '12

Photon Jets

$$D_{\rm S} \equiv \Big\{ \log\tau_1, \frac{\tau_2}{\tau_1}, \frac{\tau_3}{\tau_2}, \frac{\tau_4}{\tau_3}, \\ \big(\lambda_J, \epsilon_J, \rho_J, \delta_J\big)\big|_{\rm C/A}, \big(\lambda_J, \epsilon_J, \rho_J\big)\big|_{k_T} \Big\} \, ;$$

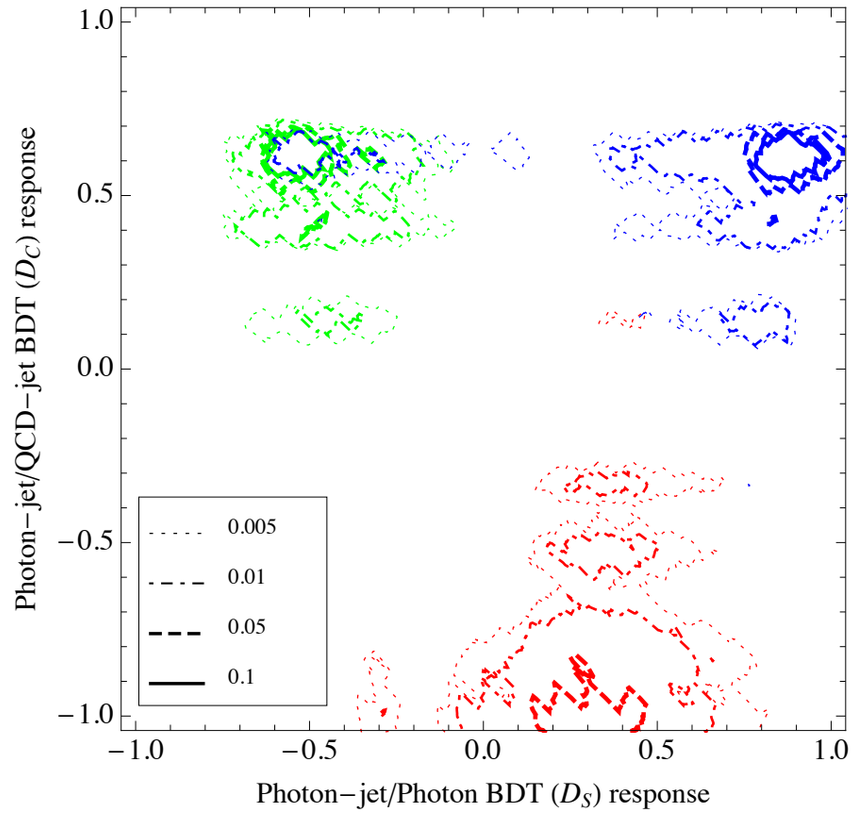

In general there are collimated electrons, photons tau which have the background

photon

electron

tau

QCD

Visualization of a space devoid of SM

Focus only on BG reduction!

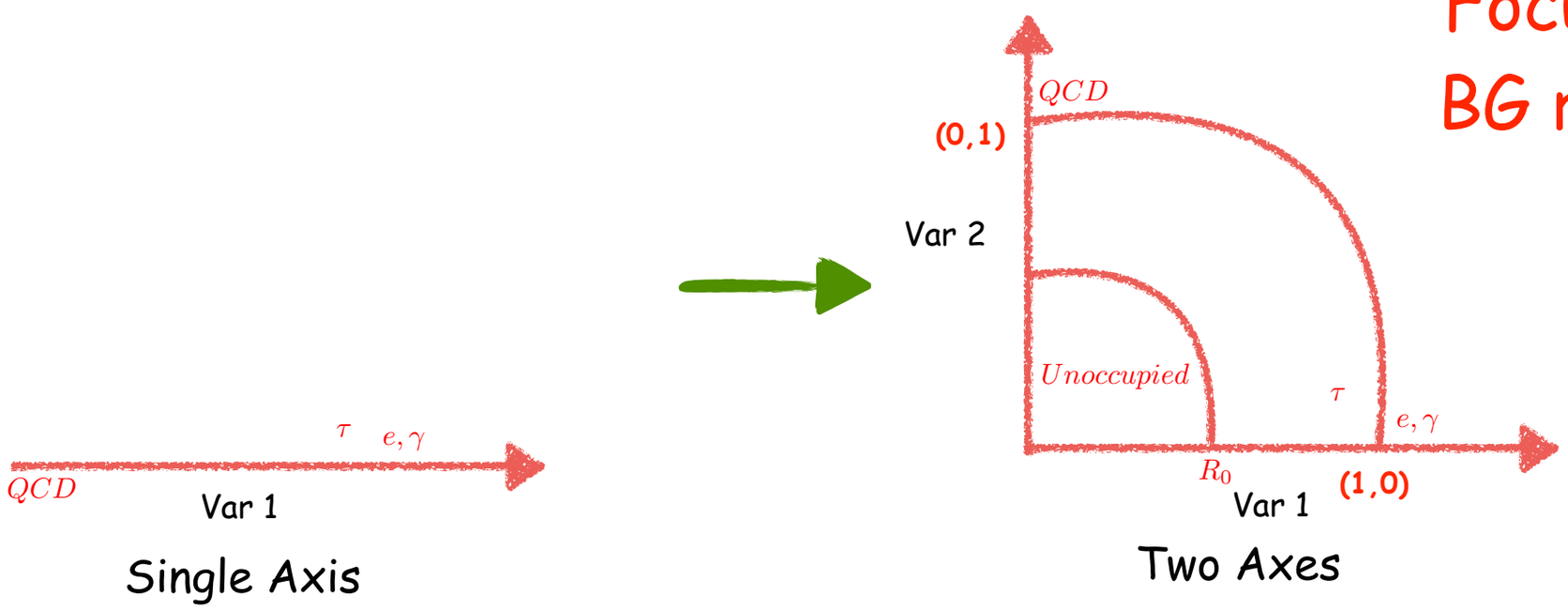

with Amit Chakrabortty and Tuhin Roy

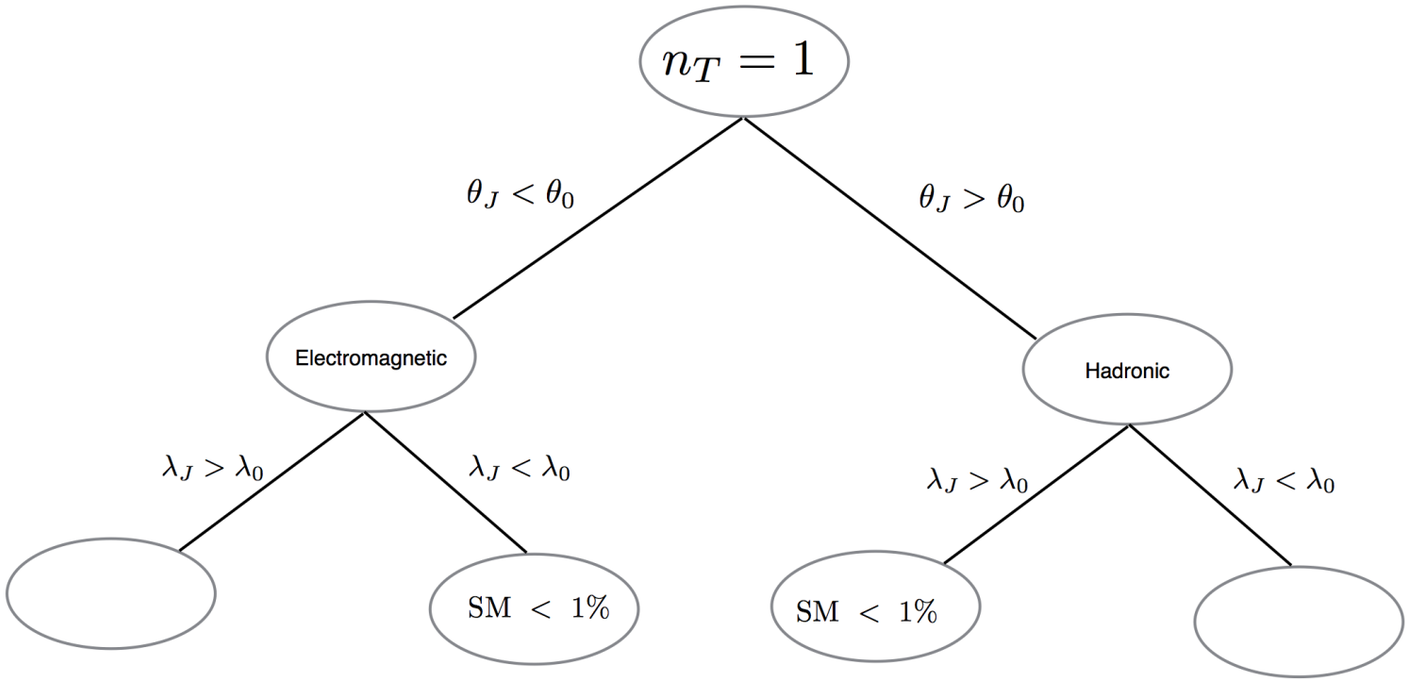

Number of Tracks	Signal Region	Selection cuts	SM backgrounds (yield in %)			
			Photon	Electron	Tau	QCD
0	SR0a	$\theta_J < -0.6, \lambda_J > -0.45$	0.3	0.09	0.196	0.03
	SR0b	$\theta_J > -0.6, \lambda_J < -1.0$	0.45	0.02	0.49	0.03
1	SR1a	$\theta_J < -0.6, \lambda_J > -0.42$	0.09	0.86	0.98	0.09
	SR1b	$\theta_J > -0.6, \lambda_J > -0.2$	0.01	0.02	0.63	0.61
2	SR2a	$\theta_J < -0.7, \lambda_J > -0.45$	0.17	0.29	0.19	0.05
	SR2b	$\theta_J > -0.7, \lambda_J < -0.65$	0.14	0.6	6.89	0.40
3	SR3a	$\theta_J < -0.5, \lambda_J > -0.4$	0.05	0.05	0.11	0.23
	SR3b	$\theta_J > -0.5, \lambda_J < -0.6$	0.04	0.003	5.22	0.72
4	SR4a	$\theta_J < -0.6$	0.08	0.2	0.05	0.11

with Amit Chakrabortty and Tuhin Roy

A toy `NP' Model

$$\mathcal{L}_{eff} \sim h G^a_{\mu\nu} G^{\mu\nu}_a + \mu_h h n_1^2 + \mu_{12} n_1 n_2^2 + (\eta_1 n_1 + \eta_2 n_2) A A,$$

$$p\ p \to h \to n_1\ n_1 \to 4\gamma, 4e, 4\tau,$$

lambdaJ

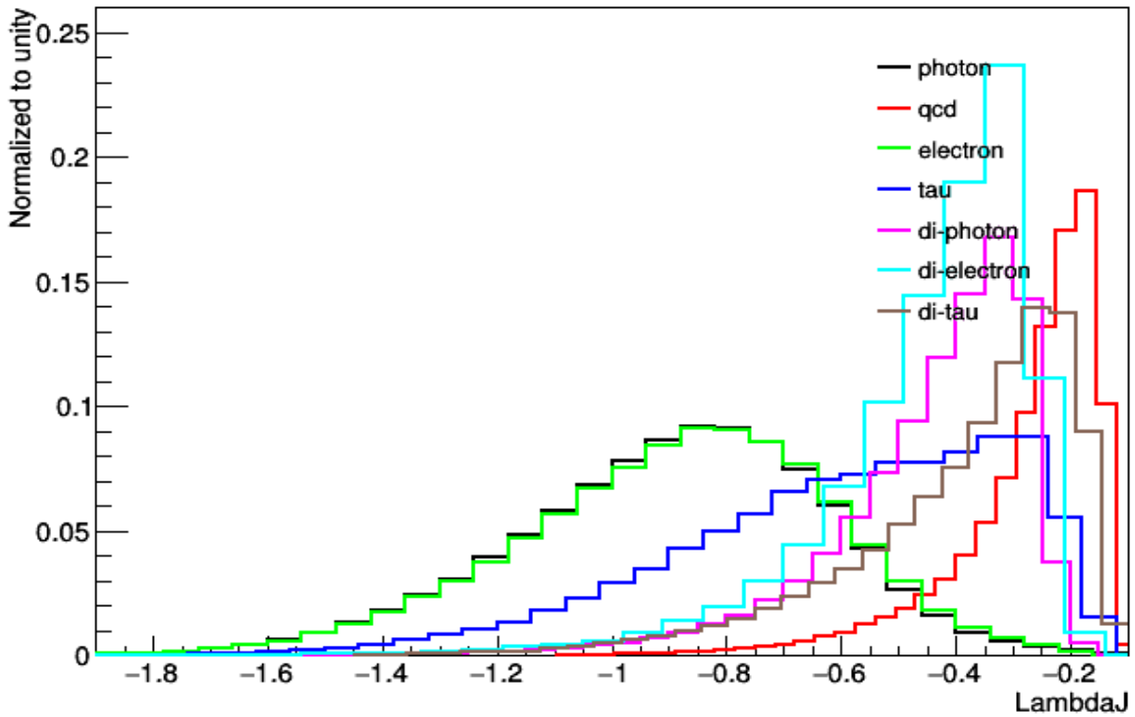

Number of Tracks	Signal Region	New Physics (yield in %)		
		Di-photon	Di-electron	Di-tau
0	SR0a	42.5	0.56	0.12
	SR0b	0.02	0	0.06
1	SR1a	11.49	6.47	0.67
	SR1b	0.06	0.03	1.02
2	SR2a	1.60	35.89	0.56
	SR2b	0.02	0.2	3.92
3	SR3a	0.41	9.11	0.63
	SR3b	0.005	0.005	2.36
4	SR4a	0.10	1.1	0.175

di-tau ~ 9% for ~ 2.4 % QCD

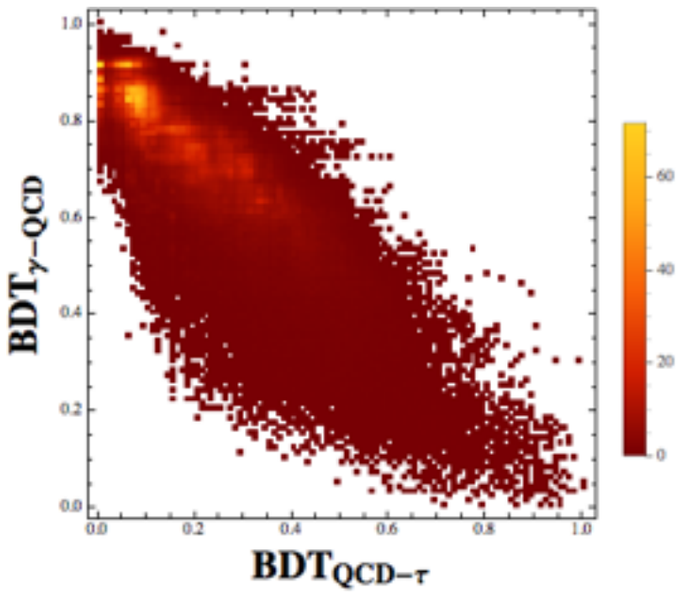

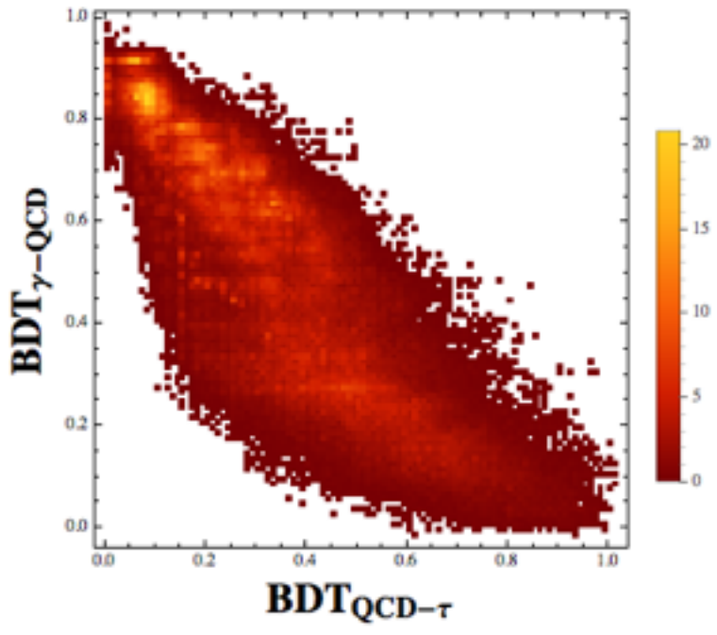

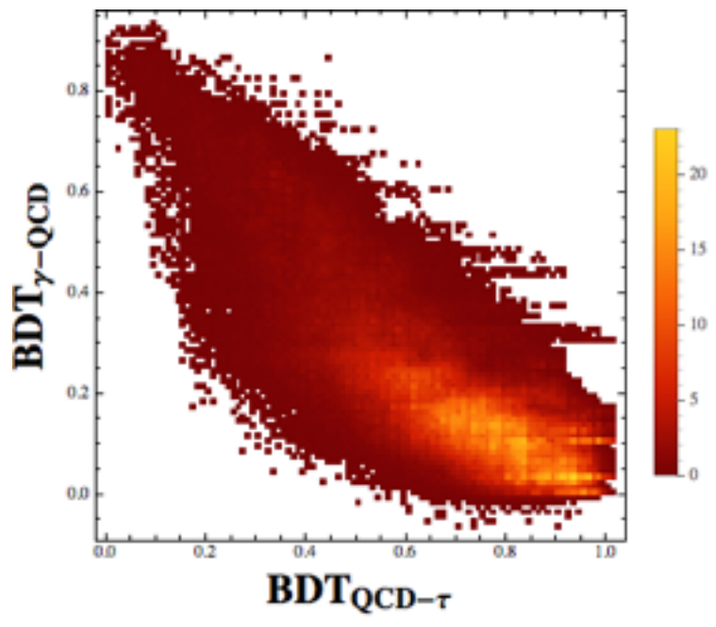

x_0 = Peak of the response distribution for the e sample

y_0 = Peak of the response distribution for the QCD sample

and define a distance function as

$$R^2 = (x - x_0)^2 + (y - y_0)^2$$

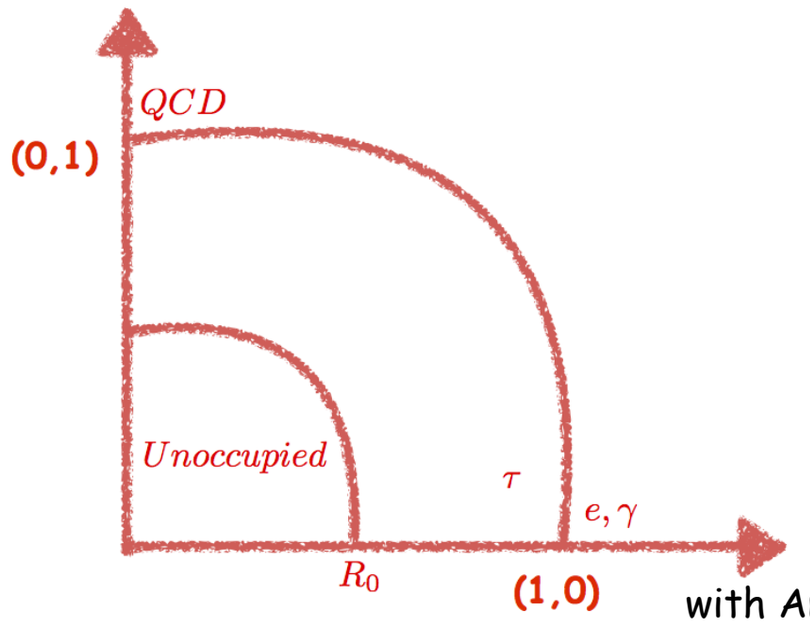

with Amit Chakrabortty and Tuhin Roy

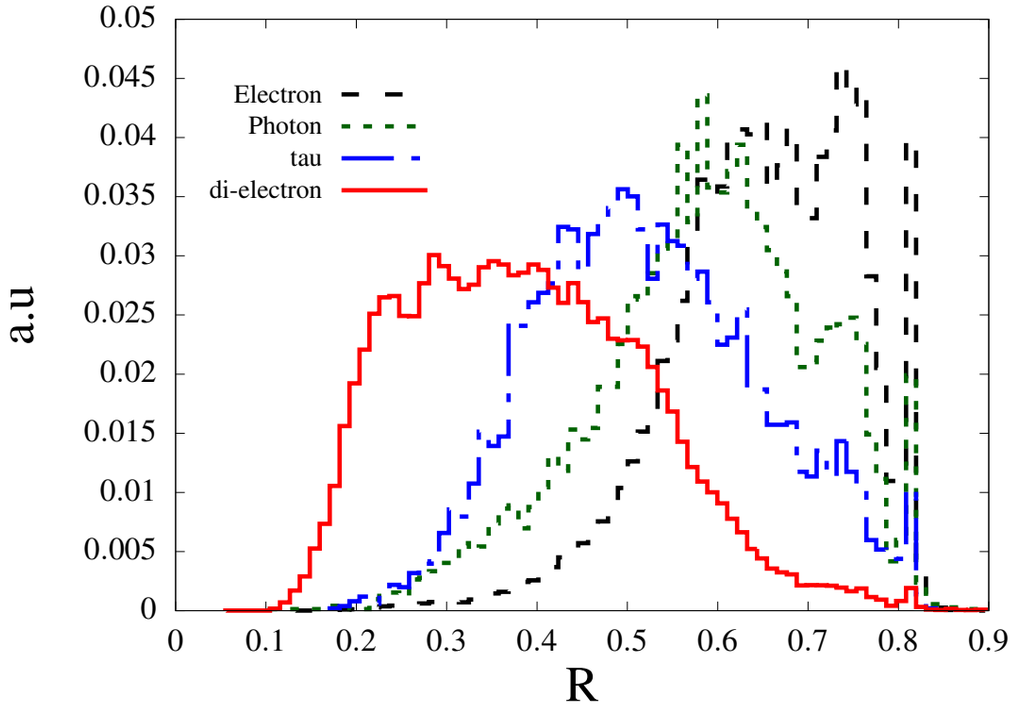

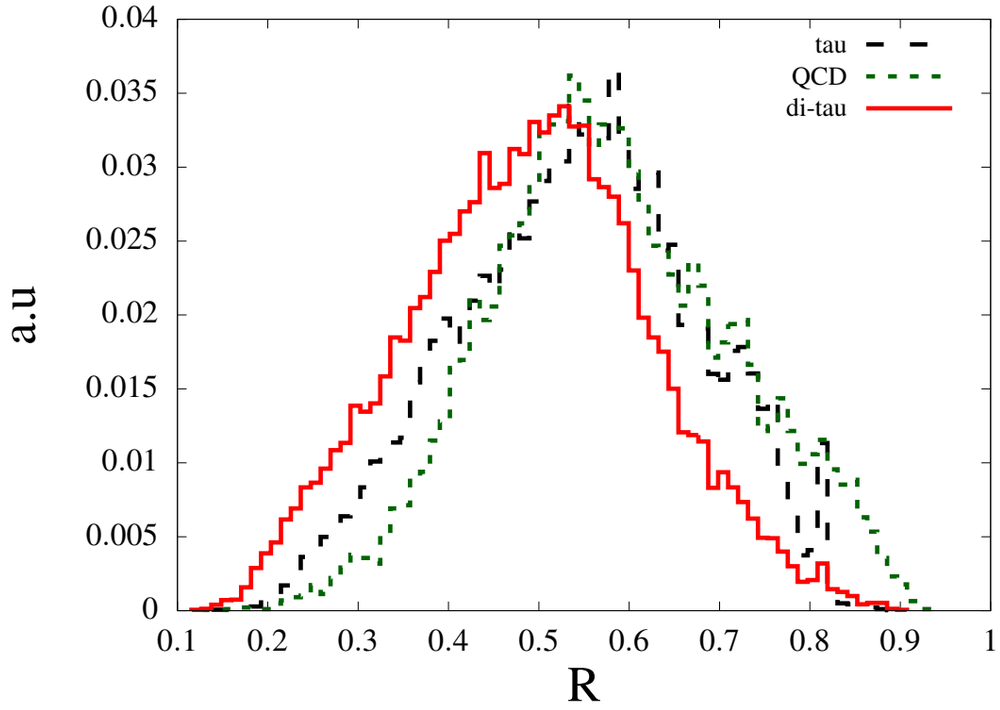

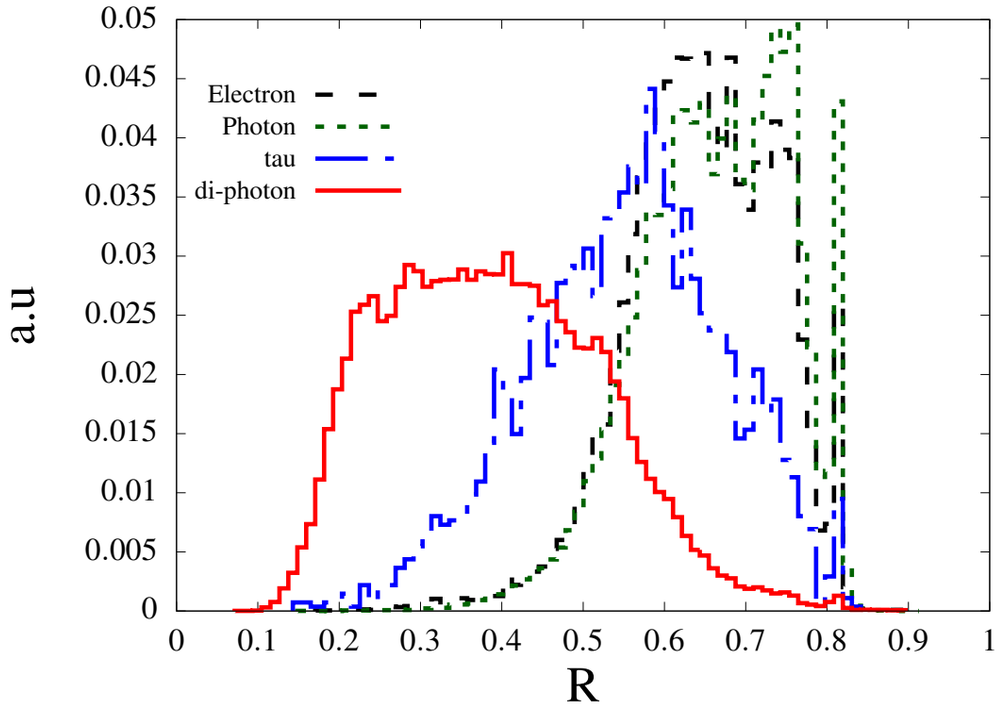

with Amit Chakrabortty and Tuhin Roy

Over to Vikram